

Alexandre François, Tess Reynolds, Nicolas Riesen, Jonathan M. M. Hall, Matthew R. Henderson, Enming Zhao, Shahraam Afshar V. and Tanya M. Monro  
**Combining whispering gallery mode lasers and microstructured optical fibers: limitations, applications and perspectives for in-vivo biosensing**  
 MRS Advances, 2016; 1(33):2309-2320

Copyright © Materials Research Society 2016

Originally Published at: <http://dx.doi.org/10.1557/adv.2016.342>

## PERMISSIONS

<http://journals.cambridge.org/action/displaySpecialPage?pageId=4608>

### Content is made freely available by the author

This is achieved by depositing the article on the author's web page or in a suitable public repository, often after a specified embargo period. The version deposited should be the Accepted Manuscript. Publishers typically impose different conditions, but it should be noted that many OA mandates (such as the NIH public access policy) specify the Accepted Manuscript in their requirements unless the publisher allows the Version of Record. Refer to the table below for details.

### Summary of where an author published in a Cambridge Journal may deposit versions of their article

STM Journals	Personal Website	Departmental / Institutional Repository	Non-commercial Subject Repository	Commercial Repository and Social Media Sites
AO	At any time	At any time	At any time	At any time
SMUR	At any time	At any time	At any time	At any time
AM	On acceptance of publication.	Six months after first publication.	Six months after first publication	Abstract only in PDF or HTML format no sooner than first publication of the full article.
VOR	Abstract only in PDF or HTML format no sooner than first publication of the full article.	Abstract only in PDF or HTML format no sooner than first publication of the full article.	Abstract only in PDF or HTML format no sooner than first publication of the full article.	Abstract only in PDF or HTML format no sooner than first publication of the full article.

1 November 2016

# Combining whispering gallery mode lasers and microstructured optical fibers: limitations, applications and perspectives for *in-vivo* biosensing

Alexandre François,<sup>1,2</sup> Tess Reynolds,<sup>2</sup> Nicolas Riesen,<sup>2</sup> Jonathan M. M. Hall,<sup>2</sup> Matthew R. Henderson,<sup>2</sup> Enming Zhao,<sup>2,3</sup> Shakraam Afshar V.<sup>1,2</sup> and Tanya M. Monro<sup>1,2</sup>

<sup>1</sup>University of South Australia, Adelaide SA 5000, Australia

<sup>2</sup>The Institute for Photonics and Advanced Sensing (IPAS), The University of Adelaide, Adelaide SA 5005, Australia

<sup>3</sup>Key Lab of In-fiber Integrated Optics, Ministry Education of China, Harbin Engineering University, China

## ABSTRACT

Whispering gallery modes (WGMs) have been widely studied over the past 20 years for various applications, including biological sensing. While the WGM-based sensing approaches reported in the literature have shown tremendous performance down to single molecule detection, at present such sensing technologies are not yet mature and still have significant practical constraints that limit their use in real-world applications. Our work has focused on developing a practical, yet effective, WGM-based sensing platform capable of being used as a dip sensor for *in-vivo* biosensing by combining WGM fluorescent microresonators with silica Microstructured Optical Fibers (MOFs).

We recently demonstrated that a suspended core MOF with a dye-doped polymer microresonator supporting WGMs positioned onto the tip of the fiber, can be used as a dip sensor. In this architecture the resonator is anchored to one of the MOF air holes, in contact with the fiber core, enabling a significant portion of the evanescent field from the fiber to overlap with the sphere and hence excite the fluorescent WGMs. This architecture allows for remote excitation and collection of the WGMs. The fiber also permits easy manipulation of the microresonator for dip sensing applications, and hence alleviates the need for a complex microfluidic interface. More importantly, it allows for an increase in both the excitation and collection efficiency compared to free space coupling, and also improves the Q factor.

In this paper we present our recent results on microstructured fiber tip WGM-based sensors and show that this sensing platform can be used in clinical diagnostics, for detecting various clinically relevant biomarkers in complex clinical samples.

## INTRODUCTION

Whispering gallery modes (WGMs) are optical resonances that occur when light is trapped by total internal reflection inside a cavity having at least one axis of revolution [1-3]. WGMs have been widely studied for various applications such as biological sensing [1, 2]. In this context, the binding of biomolecules onto the resonator surface is indirectly inferred from the shift in the resonance wavelengths occurring due to the local changes in the refractive index within the WGMs' evanescent fields. While the different WGM-based sensing approaches reported in the literature, involving either microspheres [4-8], capillaries [9-12] or toroids [13-15], have shown excellent sensing performance down to single molecule detection in pure samples [4, 13, 15, 16], this sensing approach is still in its infancy. The vast majority of work in the literature has involved passive resonators in which a phase-matched coupling strategy involving either a tapered optical fiber or a prism is required to couple light to and from the resonator [17]. To

ensure critical coupling the coupler (tapered fiber or prism) has to have a well-defined gap with the resonator. However, as shown by Zhixiong *et al.* [18], any fluctuation in the gap between the resonator and the tapered fiber or prism not only results in variations in the coupling efficiency but also causes perturbations in the resonance positions. In addition, microresonators require a microfluidic environment to be used for biosensing, adding further complexity for passive resonators if the gap between the resonator and the coupler has to be precisely maintained. A few attempts have been made to make practical the packaging of passive WGM-based sensors [19, 20], with the latest example being given in Ref [21], where a passive microsphere and a tapered optical fiber coupler were integrated on the tip of a large core fiber, effectively creating a dip sensing architecture. Despite such improvements in practicality, another critical issue remains. Throughout any biosensing experiment, biomolecules can stick to the tapered fiber coupler, inevitably altering its transmission properties, and eventually resulting in loss of the optical signal [22]. To overcome this issue, Ballard *et al.* [22] have for instance produced passive spheroidal resonators into which light can be coupled using free space optics for refractive index sensing in aqueous solution, alleviating the need for a coupler. However the performance of such a device, the Q factor in particular, is far lower than when using a standard tapered fiber coupling scheme as the free space approach requires the spheroid resonator to present a significant asymmetry or “nodes” to couple light into.

Our work using WGMs for biosensing has followed a different pathway to circumvent some of the issues mentioned above, focusing on fluorescent-based microresonators or active resonators, instead of passive ones which do not contain any gain medium [23-26]. The use of an active resonator allows for free space excitation of the WGMs via the gain medium inside the resonator. Exploiting the Purcell effect, which increases the gain medium emission within the resonator at the resonance wavelengths, allows a WGM modulated fluorescence signal to be detected in the far field. Several other research groups have also pursued the same approach in various configurations using either dye-doped microspheres [27, 28], microdroplets [29, 30], quantum dot or fluorescent nanocrystal coated microspheres [31-33], fluorescent capillaries [9, 12] and so on. Free floating active microspheres are particularly interesting due to their typically small size (i.e. 6 to 20  $\mu\text{m}$  in diameter) and it has been shown that they can be used to perform measurements within a single cell [34-36], opening new opportunities for biomedical applications. This would not be possible with passive microresonators, which are typically larger (usually  $> 50 \mu\text{m}$  in diameter) and also require a complex coupling scheme for the interrogation. Although free floating active resonators offer undeniable practical advantages, the sensing performance (i.e. detection limit) of fluorescent-based resonators has not yet reached that of passive resonators.

In this paper, we review our recent progress towards the development of a practical fluorescent microsphere based WGM sensing platform capable of being used as a dip sensor for *in-situ* biosensing applications. This is achieved by combining fluorescent microspheres with microstructured optical fibers (MOFs) [37]. We first discuss the design of the optical resonator in terms of size and refractive index to optimize its sensing properties (i.e. refractive index sensitivity and Q factor) using numerical modelling. We then experimentally demonstrate how lasing of the WGMs in the microspheres can improve the sensing performance. We also explain the reason for the lower Q factor of fluorescent-based microspheres when sampled in free space compared with tapered fiber collection, and how combining fluorescent microresonators with a suspended core microstructured optical fiber can overcome this performance limitation. We also investigate the coupling effects occurring between the microstructured optical fiber and the

active resonators, which results in an enhancement of specific modes. We conclude by presenting several examples of applications for such a sensing platform, including multiplexed sensing and dynamic self-referenced sensing. The latter allows for the detection of various biomarkers in undiluted serum, by compensating for non-specific binding events using a reference sphere in an adjacent hole of the microstructured optical fiber.

## DISCUSSION

### Optimum microsphere radius and refractive index

To optimize the sensing performance of microsphere resonators, one must determine the optimum combination of resonator diameter and refractive index. Using the model developed by Chew for the calculation of the WGM radiation from active microspheres [38, 39], we have calculated the refractive index sensitivity and Q factor as a function of the two aforementioned parameters [40]. Whilst the sensitivity is strongly enhanced when both the resonator radius and refractive index are decreased, the opposite is true for the Q factor. This is because an increase in the sensitivity necessitates an increase in the magnitude of the evanescent field, which strongly impacts the radiation loss of the propagating WGMs, resulting in lower Q factors.

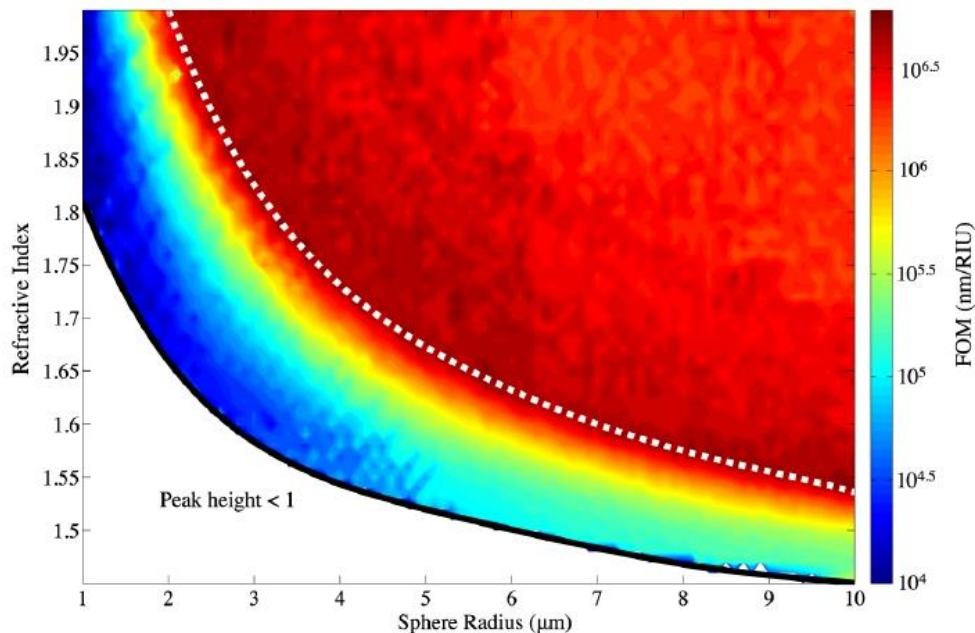


**Figure 1:** Contour plot of the figure of merit for sensing performance, defined as the product of the Q factor and the sensitivity  $S$ , as a function of the resonator radius and refractive index. The white dotted line represents the maximum value as limited by the resolution of the spectrometer assumed here to be 4 pm [40].

Using the refractive index sensitivity as a benchmark for evaluating the performance of refractive index sensing technologies can be misleading. The detection limit which describes the smallest detectable change of refractive index in the resonator's vicinity is a far more accurate metric for comparing the performance of different microresonators [41]. In order to lower the detection limit one must increase both the refractive index sensitivity and the Q factor, the latter being related to the resonator resolution. In fact, the higher the Q factor (i.e. the smaller the

linewidth of the resonance) the easier is the measurement of small wavelength shifts. However as the two parameters exhibit opposing behavior as a function of the resonator's diameter and refractive index, a tradeoff must clearly be made. Defining the figure of merit (FOM) as the product of the Q factor and the sensitivity S facilitates the analysis, although we note that in practice various noise sources will inevitably influence the detection limit [41]. Figure 1 shows the results of our FOM estimate as a function of microsphere refractive index and radius. The white dotted line shows the maximum FOM achievable, taking into account that WGM detection for active microspheres requires the use of a spectrometer which has a finite resolution (assumed to be 4 pm here). The simulation shows that for the case of polystyrene microspheres ( $n = 1.59$ ), the optimum radius is about 5  $\mu\text{m}$ .

### Polymer-based WGM microlaser

One advantage of using active resonators is the possibility of realizing stimulated emission of the gain medium within the microcavity. The Q factor being a measure of the stored energy within the resonator increases drastically as the gain overcomes the optical losses. As a consequence it is possible to reach higher Q factors when operating the resonator in the stimulated emission regime [42].

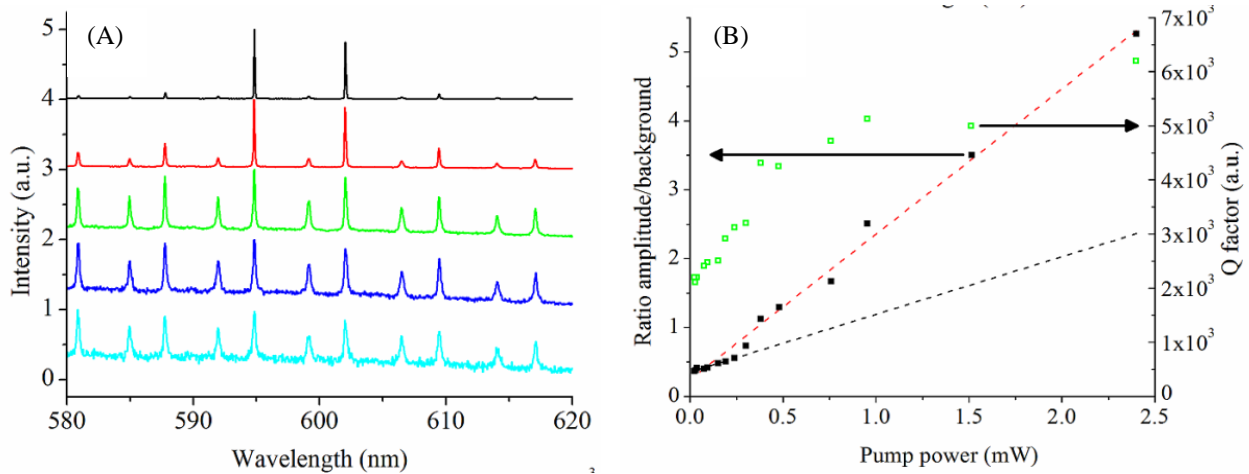


**Figure 2:** (A) Normalized WGM spectra of a 10  $\mu\text{m}$  diameter dye-doped (Nile Red) polystyrene microsphere in *water* with increasing pump power (20  $\mu\text{W}$  to 2.5 mW). (B) Measured ratio between the intensity of the dominant WGM resonance and the fluorescence background, and the Q factor, as a function of the pump power for the polystyrene microspheres in water [23].

While inducing lasing is in principle merely a matter of pumping the gain medium within the resonator with enough energy, in reality it can be a far more challenging task. The lasing threshold is a function of  $A \times V / Q^2$ , where  $V$  is the WGM mode volume and  $A$  is a gain coefficient associated with the gain medium [43]. The latter has to be kept as low as possible in order to avoid either photobleaching or photoblinking of the gain medium [44], which will affect the sensing performance and eventually prevent the lasing of the WGMs. Furthermore, the pump energy has to be kept below the damage threshold of the resonator material. Polystyrene, which is the most common material for fluorescent microspheres [2, 23-25, 28, 34-36, 40, 42, 45, 46] due to its commercial availability and ease of use, has a damage threshold of the order of 300  $\text{mJ}/\text{cm}^2$  at 532 nm [47]. We note that a high lasing threshold, even when below the actual

damage threshold of the material, may affect the resonance positions due to heating effects induced by the pump laser, introducing noise in the resonance wavelengths. The only free parameter which can be adjusted for a given active microsphere is the gain coefficient ( $A$ ), which depends on the gain medium concentration and the quantum yield. To induce lasing in  $5\ \mu\text{m}$  radius polystyrene microspheres we optimized the gain medium content to maximize the gain coefficient  $A$ , avoiding a large dye (Nile Red) concentration which would otherwise result in self-quenching [48]. With the optimized gain concentration, the  $Q$  factor was found to increase by a factor 4 from 1500 below the lasing threshold to 6000 above the lasing threshold as shown in both Figures 2 (A) and 2 (B) [23]. While lasing of the  $5\ \mu\text{m}$  radius polystyrene microspheres was achieved in water, they proved to be difficult to use for refractive index sensing due to the photobleaching mentioned above.

### Q factor limits of fluorescent microspheres

While fluorescent/active microresonators offer considerable benefits in terms of practicality as previously mentioned, their  $Q$  factors are typically several orders of magnitude lower than for passive resonators. As a result active microresonators typically exhibit reduced refractive index sensing performance. By comparing the WGM spectrum of a single fluorescent (Nile Red doped) polystyrene microsphere when using far-field and phase-matched fiber taper collection strategies, it becomes obvious that the  $Q$  factor is strongly influenced by the measurement method, as seen in the Figure 3 (A). The discrepancy in  $Q$  factor between free space and tapered fiber collection is because fiber taper collection is strongly mode-selective and collects light from only a limited subset of polar modes, while the far-field collection method collects light from almost all possible modes as illustrated in Figures 3 (C) and (D), respectively. No microsphere is ever perfectly symmetrical in practice, which induces a small perturbation in the resonance wavelengths for modes propagating in different planes/of different polar mode numbers. Since WGMs from multiple planes are collected in the far-field, a convolution of overlapping resonances is effectively measured. This results in a broadening of the resonances and hence a reduction in the  $Q$  factor for the case of far-field detection [45].

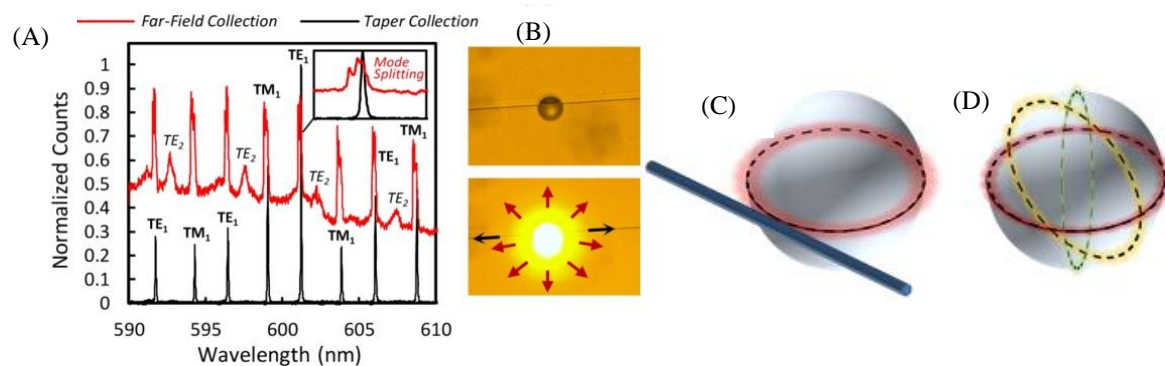


**Figure 3:** (A) Whispering gallery mode spectra sampled in the far-field (red) and via the taper (black) of the same dye-doped (Nile Red) polystyrene microsphere ( $15\ \mu\text{m}$  in diameter) excited with free space illumination. The measurements were taken simultaneously at the same pump power. Mode-splitting for far-field collection is shown in the inset. (B) Microscope images showing the taper and attached microsphere under free space excitation. Depiction of the (C) fiber taper and (D) far-field collection strategies [45].

## Combining fluorescent microsphere resonators with suspended core microstructured optical fibers

The first attempt at combining fluorescent microsphere resonators with suspended core microstructured optical fibers was motivated by the idea that the optical fiber could be used to guide the pump source to the microsphere and simultaneously collect the WGM modulated fluorescence, effectively creating a robust dip sensing platform which we envisioned could be used for *in-vivo* sensing applications [26]. In this context a fluorescent polystyrene microsphere was simply attached to the tip of a microstructured optical fiber, exploiting the electrostatic repulsion between the negatively charged surfaces of both the fiber tip and the polystyrene microsphere, to anchor the resonator into one of the MOF's holes. The microsphere used typically being larger than the MOF's holes, ensures that the resonator doesn't fully penetrate inside the MOF, unlike work by other research groups [49-51]. Instead the microsphere protrudes out of the MOF's tip leaving a large portion of the resonator exposed to the outside environment allowing it to serve as a sensor. While the refractive index sensitivity of the resonator was not affected in the process, the Q factor was significantly lowered when both the excitation and collection of the WGM signal was performed through the high refractive index lead silicate MOF ( $n=1.69$ ) [26].

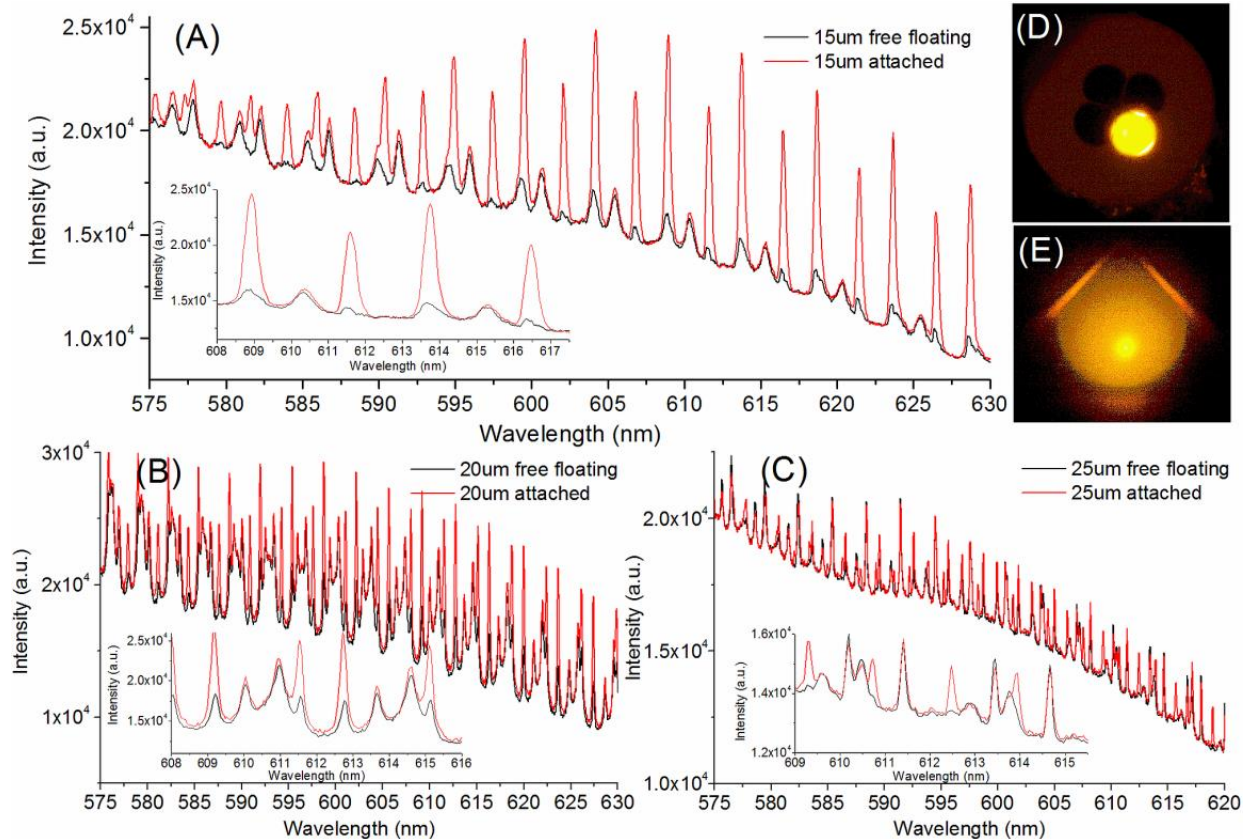


**Figure 4:** Whispering gallery mode spectra of dye-doped (Nile Red) polystyrene microspheres with a nominal diameter of (A) 15 μm, (B) 20 μm and (C) 25 μm, either free floating or positioned into a hole of the suspended core microstructured optical fiber ( $\varnothing_{\text{hole}} = 17 \mu\text{m}$ ). (D) and (E) are images of a fluorescing sphere [25].

As an extension of this initial work, we investigated the coupling between the active microsphere and the MOF host as a function of the diameter mismatch between the fiber hole and the resonator. A comparison of the WGM modulated fluorescence spectra for microspheres with different diameters: 15, 20 and 25  $\mu\text{m}$ , before and after being attached onto a silica MOF tip ( $\text{O}_{\text{hole}} = 17 \mu\text{m}$ ), is presented in Figures 4 (A), (B) and (C), respectively. From these spectra, it becomes obvious that upon immobilization of the microsphere onto the MOF tip, Transverse Electric (TE) polarized resonances are greatly enhanced. The magnitude of the enhancement is a function of the diameter mismatch between the microsphere and the MOF hole in which it resides. Numerical modelling conducted using the MIT *MEEP* FDTD solver [52], revealed that the physical origins of this effect could involve: a ‘lensing’ effect, where the high refractive index of the glass refracts the radiated light; increased out-coupling of light from the resonator due to the presence of the high-index medium, as exploited in prism coupling with microresonators [53]; and/or scattering and reflection of the evanescent field at the water-glass interface. Indeed, these effects could explain the ‘bright spots’ observed experimentally at the points where the microsphere touches the surrounding glass fiber as shown in Figure 4 (E). The FDTD analysis however did not reveal the nature of the polarization dependent enhancement (TE vs TM), and to date the physical reasons remain unclear. For the case of the TE modes the enhancement in Q factor is  $\sim 30\%$  for both the fluorescence and stimulated emission regimes, when the microsphere diameter matches the fiber’s hole diameter. We believe that in this particular configuration, the coupling between the microsphere and the microstructured fiber behaves similarly to that of a passive microsphere and a tapered optical fiber, enabling the selective collection of a smaller number of polar modes, alleviating at least partially the influence of the intrinsic microsphere asphericity on Q factor as shown in the previous section.

### **Dip sensing architecture: Improving the performance with lasing microspheres**

Having realized these improvements in performance, we proceeded to use a well-known specific interaction model based on the biotin/Neutravidin system to investigate the benefits of inducing *lasing* in microspheres on the tip of suspended core MOFs for biosensing [24]. The experimental setup is depicted in Figure 5 (A) where the MOF/microsphere combination is used as a dip sensor, alleviating the need for a microfluidic flow cell. The microspheres were surface functionalized in bulk with polyelectrolyte layers [54], providing amine moieties for subsequent covalent immobilization of biotin which presents one carboxylic function using carboxyl to amine coupling carbodiimide chemistry. Non-specific binding sites were blocked with casein.

Once a batch of microspheres was functionalized, one of the spheres was attached to the tip of the suspended core MOF, before the fiber was dipped into a Neutravidin solution in Phosphate Buffer Saline (pH 7.4) with a concentration ranging from 4 nM to 1600 nM. The binding kinetics for the microspheres below and above the lasing threshold are shown in Figures 5 (B) and (C), respectively. From the figures 5 (B) and (C) it becomes obvious that while the sensitivity is not increased by the lasing operation, the resolution, i.e. the smallest wavelength shift detectable, is improved due to the increase in Q factor. As a result, the lasing operation allows for a reduction in the uncertainty of the resonance wavelength. This enables the detection of smaller Neutravidin concentrations with lasing microspheres down to 4 nM, which was not possible with the non-lasing microspheres.

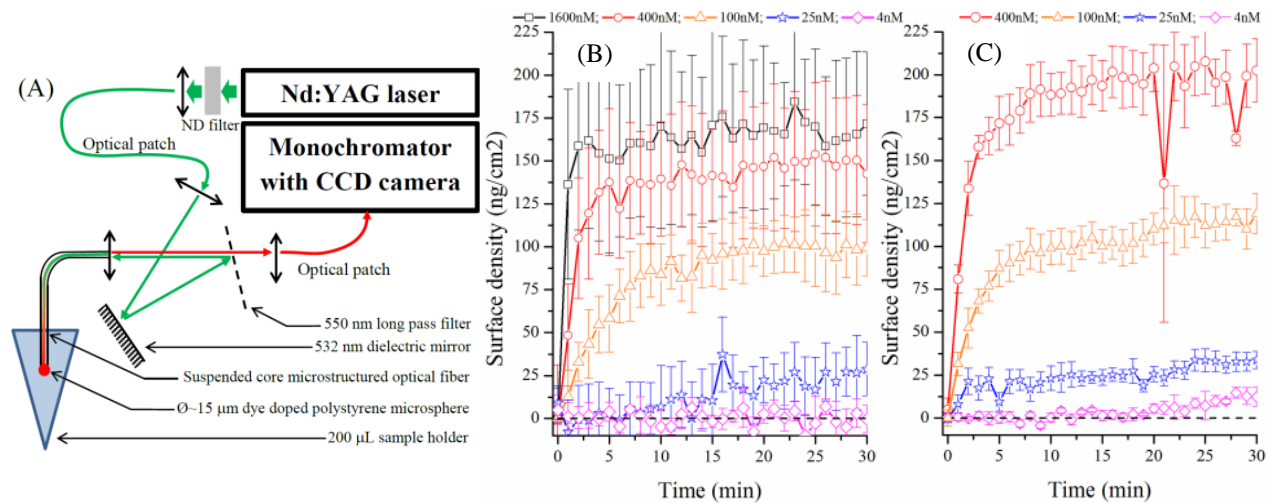


**Figure 5:** (A) Schematic of the optical setup. Binding kinetic for Neutravidin (4 nM - 1600 nM) on a  $\varnothing = 20 \mu\text{m}$  biotin functionalized sphere operated (B) below and (C) above the lasing threshold [24].

### **Biosensing applications: Dynamic self-referenced and multiplexed sensing**

While most of the biosensing demonstrations using WGM sensing platforms that are reported in the literature are performed in pure solution, *i.e.* target proteins in salt buffer solution, clinical application requires the detection to be done in complex biological samples such as serum, urine, saliva and so on. However, like all refractive index based sensing technologies, WGM sensing platforms are plagued by non-specific binding, which leads to false positive readings when they are used in such complex samples. This limits the prospects for such technologies to be used as biomedical diagnostic instruments, beyond the more controlled research laboratory environment. While a lot of effort has been dedicated to overcoming this issue by developing non-fouling coatings to prevent unwanted interactions from occurring, their applicability is strongly dependent on the substrate. The best example in this regard is the development of thiol terminated Poly Ethylene Glycol (PEG) which forms self-assembled comb-like structures, efficiently preventing non-specific binding in serum, on gold and silver substrates used for another very successful refractive index sensing platform: Surface Plasmon Resonance [55]. Recent work by Soteropoulos *et al.* [56], has reported the use of a similar silane terminated PEG layer formation strategy on silica microspheres for limiting non-specific binding, although an unambiguous demonstration of the performance of such surface coatings in serum has not been achieved. Another approach for limiting non-specific binding is to dilute the sample (*i.e.* serum) in order to minimize its impact [8]. However, diluting the sample may affect the viability of the detection for some applications where the concentration of the analyte to be detected may already be close to the detection limit.

Our approach to solving this issue is transformational. It relies on using two almost identical microspheres, ideally differing only in how their surfaces are functionalized. The microspheres are positioned onto the tip of a single MOF and therefore are subjected to the same local environment. Operating both resonators at the same wavelength ensures that they have similar refractive index sensitivity, and inducing lasing of both resonators enables the resonances of the two microspheres to be easily distinguished due to the increase in Q factor which results in very narrow linewidths. One microsphere (*i.e.* sensing resonator) is functionalized in such a way that

it preferentially interacts with the analyte to be detected using an antibody to warrant the specific nature of the interaction, while the second microsphere (*i.e.* reference resonator) has its surface passivated with standard blocking proteins, such as casein, and measures the non-specific binding as well as any other changes in the local environment that may induce a wavelength shift, such as temperature fluctuations. The second microsphere is, in that case, effectively used as a floating reference. The ability of this two microsphere sensing strategy to perform measurements in undiluted serum was evaluated using the biotin/Neutravidin model described in the previous section. Undiluted human serum samples, deprived of immunoglobulin which can bind to biotin, spiked with different Neutravidin concentrations were used and compared with Neutravidin in PBS solutions of the same concentration. Figure 6 shows the binding kinetics for 50, 25 and 5 nM Neutravidin in both PBS and serum for both the sensing and reference resonators. These results demonstrate that this simple approach based on using multiple microresonators can efficiently compensate for non-specific binding in complex biological samples without compromising the sensitivity level.

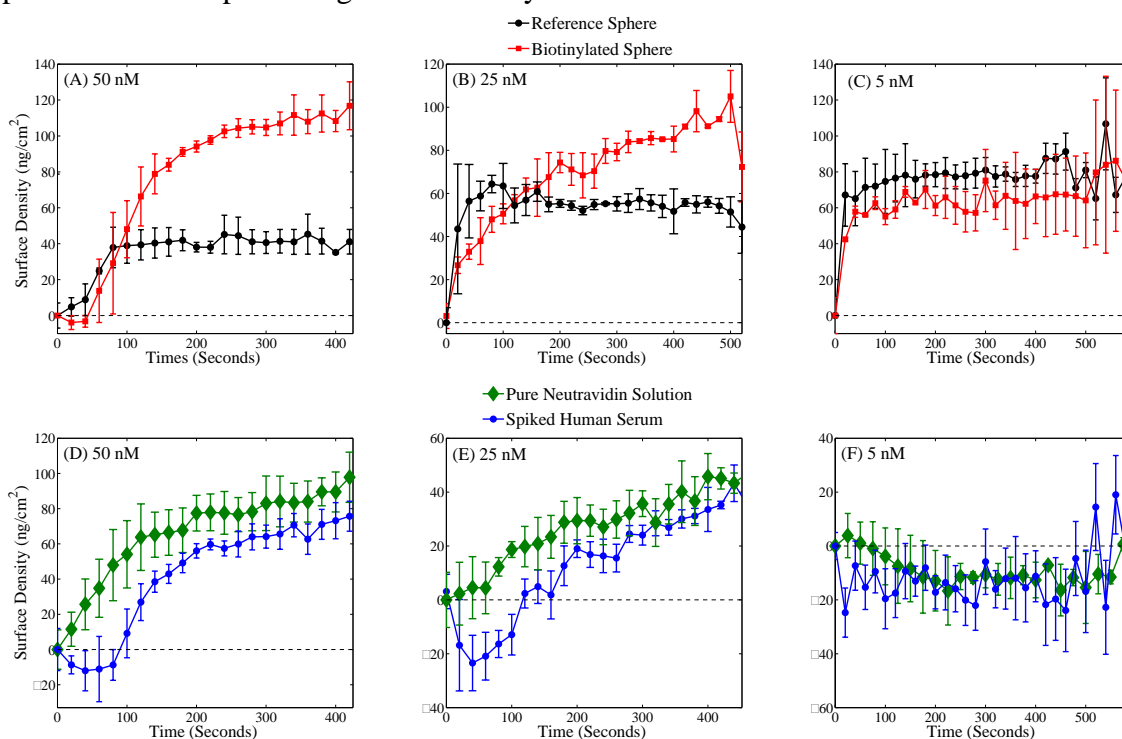


**Figure 6:** Individual sphere responses of the biotinylated (red trace) and reference (black trace) spheres when dipped into human serum samples spiked with (A) 50 nM, (B) 25 nM and (C) 5 nM concentrations of Neutravidin. (D)-(F) Comparison of the corrected binding kinetic of the sensor in the spiked human serum samples (blue trace) with binding kinetic in the pure Neutravidin solutions (green trace). Reprinted with permission from T. Reynolds, A. François, N. Riesen, M. E. Turvey, S. J. Nicholls, P. Hoffman, and T. M. Monro, *Anal. Chem.* **88**, 4036-4040 (2016). Copyright (2016) American Chemical Society.

The current trend for early stage diagnostics, especially for cancer, has evolved towards the detection of multiple biomarkers simultaneously rather than a single one with the ultimate goal being to evaluate how their concentrations deviate from their normal regulation ranges [57-60]. Therefore being able to detect and quantify a select panel of biomarkers simultaneously is of

high interest. Multiplexed detection of 2 different biomolecules with a WGM sensor was first demonstrated by Vollmer *et al.* [61], using passive resonators. However, the realization of such a sensing device, requiring two different passive microspheres to be coupled to the same tapered fiber, is particularly cumbersome and the potential for expanding this concept to a higher number of biomolecules to be detected is limited. Multiplexed detection using fluorescent microspheres is reported in Ref. [62]. However the authors used microspheres with different sizes, and therefore different sensitivities. Our approach of using multiple identical lasing microspheres to compensate for non-specific binding can easily be adapted to multiplexed sensing applications without having to vary the microsphere's size or to use different gain media to differentiate the signals emerging from the different microspheres. The number of different biomolecules which could be detected simultaneously is only limited by the fiber architecture which dictates the maximum number of resonators that could be attached onto its tip.

## CONCLUSIONS

In this work, we have discussed novel dip sensing architectures that are based on combining fluorescent microspheres supporting WGMs with suspended core MOFs. Identifying the limiting factor on the Q factor of fluorescent microspheres, which is often the inherent low-level asphericity, has allowed us to further understand the constraints of this approach. More importantly, this has allowed us to appreciate the benefit of using suspended core MOFs for both exciting and collecting the WGM modulated fluorescence signals from active microspheres as it avoids the Q factor spoiling occurring when using far-field sampling. Modelling of the WGMs in fluorescent microspheres has allowed us to map out the refractive index sensitivity and Q factor as functions of both the microsphere refractive index and diameter. This has revealed that for a particular resonator refractive index there exists a specific diameter which has an optimal tradeoff between sensitivity and Q factor, and hence optimizes the detection limit. For commercially available polystyrene microspheres, this optimum diameter was found to be approximately 10  $\mu\text{m}$ . Having understood the advantage of inducing lasing of the WGMs in microresonators for enhancing the Q factors, we proceeded to demonstrate lasing of a 10  $\mu\text{m}$  diameter polystyrene microsphere in aqueous solution for the first time, by carefully tuning the amount of gain medium within the resonator. We demonstrated that our approach of using lasing fluorescent microspheres on the tip of a MOF can be used for biosensing applications and that using multiple microspheres on the tip enables the compensation of the WGM wavelength shift associated with non-specific binding in undiluted serum. This was made possible by adopting a multiplexed sensing strategy where one microsphere was functionalized to detect a specific biomolecule while a second microsphere was treated to only measure changes in the surrounding environment and non-specific binding. Expanding this strategy further could allow for multiplexed sensing in clinical samples never before achieved using WGMs.

## ACKNOWLEDGMENTS

T. M. Monro acknowledges the support of an ARC Georgina Sweet Laureate Fellowship. This work was performed in part at the Optofab node of the Australian National Fabrication Facility utilizing Commonwealth and SA State Government funding.

## REFERENCES

- 1 M. R. Foreman, J. D. Swaim, and F. Vollmer, *Adv. Opt. Photon.* **7**, 168-240 (2015).
- 2 A. François, Y. Zhi, and A. Meldrum, in *Photonic Materials for Sensing, Biosensing and Display Devices*, edited by M. J. Serpe, Y. Kang and Q. M. Zhang (Springer, 2016), p. 237-288.
- 3 A. Chiasera, Y. Dumeige, P. Féron, M. Ferrari, Y. Jestin, G. N. Conti, S. Pelli, S. Soria, and G. C. Righini, *Laser Photon. Rev.* **4**, 457-482 (2010).
- 4 M. D. Baaske, M. R. Foreman, and F. Vollmer, *Nat. Nanotechnol.* **9**, 933-939 (2014).
- 5 H.-C. Ren, F. Vollmer, S. Arnold, and A. Libchaber, *Opt. Express* **15**, 17410-17423 (2007).
- 6 F. Vollmer, S. Arnold, and D. Keng, *Proc. Natl. Acad. Sci. U S A* **105**, 20701-20704 (2008).
- 7 F. Vollmer and S. Arnold, *Nat. Methods* **5**, 591-596 (2008).
- 8 L. Pasquardini, et al., *J. Biophoton.* **6**, 178-187 (2013).
- 9 S. Lane, P. West, A. François, and A. Meldrum, *Opt. Express* **23**, 2577-2590 (2015).
- 10 X. D. Fan and I. M. White, *Nat. Photon.* **5**, 591-597 (2011).
- 11 I. White, H. Zhu, J. Suter, X. Fan, and M. Zourob, in *Biosensors and Biodetection*, edited by A. Rasooly and K. Herold (Humana Press, 2009), Vol. 503, p. 139-165.
- 12 K. J. Rowland, A. François, P. Hoffmann, and T. M. Monroe, *Opt. Express* **21**, 11492-11505 (2013).
- 13 J. Zhu, S. K. Ozdemir, Y.-F. Xiao, L. Li, L. He, D.-R. Chen, and L. Yang, *Nat. Photon.* **4**, 46-49 (2010).
- 14 D. K. Armani, T. J. Kippenberg, S. M. Spillane, and K. J. Vahala, *Nature* **421**, 925-928 (2003).
- 15 J. Su, A. F. G. Goldberg, and B. M. Stoltz, *Light Sci. Appl.* **5**, e16001 (2016).
- 16 L. Shao, X.-F. Jiang, X.-C. Yu, B.-B. Li, W. R. Clements, F. Vollmer, W. Wang, Y.-F. Xiao, and Q. Gong, *Adv. Mater.* **25**, 5616-5620 (2013).
- 17 G. C. Righini, Y. Dumeige, P. Féron, M. Ferrari, G. N. Conti, D. Ristic, and S. Soria, *Riv. Nuovo Cimento* **34**, 435-488 (2011).
- 18 G. Zhixiong, Q. Haiyong, and P. Stanley, *J. Phys. D Appl. Phys.* **39**, 5133-5136 (2006).
- 19 P. Wang, M. Ding, G. S. Murugan, L. Bo, C. Guan, Y. Semenova, Q. Wu, G. Farrell, and G. Brambilla, *Opt. Lett.* **39**, 5208-5211 (2014).
- 20 K. Scholten, X. Fan, and E. T. Zellers, *Lab Chip* **14**, 3873-3880 (2014).
- 21 M. Agarwal and I. Teraoka, *Anal. Chem.* **87**, 10600-10604 (2015).
- 22 Z. Ballard, M. Baaske, and F. Vollmer, *Sensors* **15**, 8968-8980 (2015).
- 23 A. François, N. Riesen, H. Ji, S. V. Afshar, and T. M. Monroe, *Appl. Phys. Lett.* **106**, 031104 (2015).
- 24 A. François, T. Reynolds, and T. Monroe, *Sensors* **15**, 1168-1181 (2015).
- 25 A. François, K. J. Rowland, S. V. Afshar, M. R. Henderson, and T. M. Monroe, *Opt. Express* **21**, 22566-22577 (2013).
- 26 A. François, K. J. Rowland, and T. M. Monroe, *Appl. Phys. Lett.* **99**, 141111 (2011).
- 27 E. Nuhiji and P. Mulvaney, *Small* **3**, 1408-1414 (2007).
- 28 M. Himmelhaus, S. Krishnamoorthy, and A. François, *Sensors* **10**, 6257-6274 (2010).
- 29 A. I. El Abed and V. Taly, *Opt. Mater.* **36**, 64-68 (2013).
- 30 V. D. Ta, R. Chen, and H. D. Sun, *Sci. Rep.* **3**, 1362 (2013).
- 31 N. V. Kryzhanovskaya, M. V. Maximov, and A. E. Zhukov, *Quant. Electron.* **44**, 189-200 (2014).

- 32 A. V. Veluthandath and P. B. Bisht, *J. Appl. Phys.* **118**, 233102 (2015).
- 33 Y. Zhi, J. Valenta, and A. Meldrum, *JOSA B* **30**, 3079-3085 (2013).
- 34 M. Himmelhaus and A. François, *Biosens. Bioelectron.* **25**, 418-427 (2009).
- 35 M. Humar and S. Hyun Yun, *Nat. Photon.* **9**, 572-576 (2015).
- 36 M. Schubert, A. Steude, P. Liehm, N. M. Kronenberg, M. Karl, E. C. Campbell, S. J. Powis, and M. C. Gather, *Nano. Lett.* **15**, 5647-5652 (2015).
- 37 T. M. Monro, S. Warren-Smith, E. P. Schartner, A. François, S. Heng, H. Ebendorff-Heidepriem, and S. Afshar V, *Opt. Fiber Technol.* **16**, 343-356 (2010).
- 38 H. Chew, *J. Chem. Phys.* **87**, 1355-1360 (1987).
- 39 H. Chew, *Phys. Rev. A* **38**, 3410-3416 (1988).
- 40 T. Reynolds, M. R. Henderson, A. François, N. Riesen, J. M. M. Hall, S. V. Afshar, S. J. Nicholls, and T. M. Monro, *Opt. Express* **23**, 17067-17076 (2015).
- 41 I. M. White and X. Fan, *Opt. Express* **16**, 1020-1028 (2008).
- 42 A. François and M. Himmelhaus, *Appl. Phys. Lett.* **94**, 031101 (2009).
- 43 S. M. Spillane, T. J. Kippenberg, and K. J. Vahala, *Nature* **415**, 621-623 (2002).
- 44 J. Schuster, J. Brabandt, and C. von Borczyskowski, *JOL* **127**, 224-229 (2007).
- 45 N. Riesen, T. Reynolds, A. François, M. R. Henderson, and T. M. Monro, *Opt. Express* **23**, 28896-28904 (2015).
- 46 T. Reynolds, A. François, N. Riesen, M. E. Turvey, S. J. Nicholls, P. Hoffman, and T. M. Monro, *Anal. Chem.* **88**, 4036-4040 (2016).
- 47 J. Venturini, E. Koudoumas, S. Couris, J. M. Janot, P. Seta, C. Mathis, and S. Leach, *J. Mater. Chem.* **12**, 2071-2076 (2002).
- 48 M. Akbulut, P. Ginart, M. E. Gindy, C. Theriault, K. H. Chin, W. Soboyejo, and R. K. Prud'homme, *Adv. Funct. Mater.* **19**, 718-725 (2009).
- 49 K. Kosma, G. Zito, K. Schuster, and S. Pissadakis, *Opt. Lett.* **38**, 1301-1303 (2013).
- 50 H. Li, S. Hao, L. Qiang, J. Li, and Y. Zhang, *Appl. Phys. Lett.* **102**, 231908 (2013).
- 51 W. Lin, H. Zhang, B. Liu, B. Song, Y. Li, C. Yang, and Y. Liu, *Sci. Rep.* **5**, 17791 (2015).
- 52 A. F. Oskooi, D. Roundy, M. Ibanescu, P. Bermel, J. D. Joannopoulos, and S. G. Johnson, *Comp. Phys. Commun.* **181**, 687-702 (2010).
- 53 A. N. Oraevsky, *Quant. Electron.* **32**, 377-400 (2002).
- 54 G. Decher, *Science* **277**, 1232-1237 (1997).
- 55 O. R. Bolduc, J. N. Pelletier, and J.-F. Masson, *Anal. Chem.* **82**, 3699-3706 (2010).
- 56 C. E. Soteropoulos, K. M. Zurick, M. T. Bernards, and H. K. Hunt, *Langmuir* **28**, 15743-15750 (2012).
- 57 K. R. Kozak, F. Su, J. P. Whitelegge, K. Faull, S. Reddy, and R. Farias-Eisner, *Proteomics* **5**, 4589-4596 (2005).
- 58 M. F. Buas, H. Gu, D. Djukovic, J. Zhu, C. W. Drescher, N. Urban, D. Raftery, and C. I. Li, *Gynecol. Oncol.* **140**, 138-144 (2016).
- 59 S. Spindel and K. Sapsford, *Sensors* **14**, 22313-22341 (2014).
- 60 J. M. Humphries, M. A. S. Penno, F. Weiland, M. Klingler-Hoffmann, A. Zuber, A. Boussioutas, M. Ernst, and P. Hoffmann, *BBA-Proteins Proteom.* **1844**, 1051-1058 (2014).
- 61 F. Vollmer, S. Arnold, D. Braun, I. Teraoka, and A. Libchaber, *Biophys. J.* **85**, 1974-1979 (2003).
- 62 H. A. Huckabay and R. C. Dunn, *Sensor. Actuat. B-Chem.* **160**, 1262-1267 (2011).